FERMILAB-PUB-19-525-AE-PPD-SCD

Prepared for submission to JHEP

Light vector mediator search in the low-energy data of the CONNIE reactor neutrino experiment

CONNIE Collaboration

Alexis Aguilar-Arevalo,[a] Xavier Bertou,[b] Carla Bonifazi,[c] Gustavo Cancelo,[d] Brenda Aurea Cervantes-Vergara,[a,1] Claudio Chavez,[e] Juan C. D'Olivo,[a] João C. dos Anjos,[f] Juan Estrada,[d] Aldo R. Fernandes Neto,[g] Guillermo Fernandez-Moroni,[d,h] Ana Foguel,[c] Richard Ford,[d] Federico Izraelevitch,[i] Ben Kilminster,[j] H. P. Lima Jr,[f] Martin Makler,[f] Jorge Molina,[e] Philipe Mota,[f] Irina Nasteva,[c] Eduardo Paolini,[h] Carlos Romero,[e] Youssef Sarkis,[a] Miguel Sofo Haro,[b] Javier Tiffenberg,[d] and Christian Torres.[e]

[a] *Universidad Nacional Autónoma de México, Distrito Federal, México*

[b] *Centro Atómico Bariloche and Instituto Balseiro, Comisión Nacional de Energía Atómica (CNEA), Consejo Nacional de Investigaciones Científicas y Técnicas (CONICET), Universidad Nacional de Cuyo (UNCUYO), San Carlos de Bariloche, Argentina.*

[c] *Universidade Federal do Rio de Janeiro, Instituto de Física, Rio de Janeiro, RJ, Brazil*

[d] *Fermi National Accelerator Laboratory, Batavia, IL, United States*

[e] *Facultad de Ingeniería - Universidad Nacional de Asunción, Asunción, Paraguay*

[f] *Centro Brasileiro de Pesquisas Físicas, Rio de Janeiro, RJ, Brazil*

[g] *Centro Federal de Educação Tecnológica Celso Suckow da Fonseca, Angra dos Reis, RJ, Brazil*

[h] *Instituto de Investigaciones en Ingeniería Eléctrica, Departamento de Ingeniería Eléctrica y Computadoras, Universidad Nacional del Sur (UNS) - CONICET, Bahía Blanca, Argentina*

[i] *Universidad Nacional de San Martín (UNSAM), Comisión Nacional de Energía Atómica (CNEA), Consejo Nacional de Investigaciones Científicas y Técnicas (CONICET), Argentina*

[j] *Universität Zürich Physik Institut, Zurich, Switzerland*

Abstract: The CONNIE experiment is located at a distance of 30 m from the core of a commercial nuclear reactor, and has collected a 3.7 kg-day exposure using a CCD detector array sensitive to an $\sim$1 keV threshold for the study of coherent neutrino-nucleus elastic scattering. Here, we use the results previously published by the CONNIE collaboration to constrain the allowed region in the parameter space of a Standard Model extension with a light vector mediator. We obtain new world-leading constraints for a light vector mediator with mass $M_{Z'} < 10$ MeV. These results constitute the first use of the CONNIE data as a probe for physics beyond the Standard Model.

[1] Corresponding author: bren.cv@ciencias.unam.mx

This document was prepared by [CONNIE Collaboration] using the resources of the Fermi National Accelerator Laboratory (Fermilab), a U.S. Department of Energy, Office of Science, HEP User Facility. Fermilab is managed by Fermi Research Alliance, LLC (FRA), acting under Contract No. DE-AC02-07CH11359

Contents

1 Introduction 1

2 Event rate in CONNIE 2

3 Search for light vector mediator using CONNIE data 4

4 Conclusion 5

A Reactor flux 6

B Fitting functions for quenching factor and efficiency 8

1 Introduction

Coherent Elastic Neutrino-Nucleus Scattering (CEνNS) is a Standard Model (SM) process predicted more than 40 years ago [1] where a neutrino interacts coherently with all nucleons present in an atomic nucleus, resulting in an enhancement of the scattering cross section. The enhancement is approximately proportional to the square of the number of neutrons in the nucleus. However, despite its large cross section, this process took a long time to be observed due to the difficulty of measuring the low-energy nuclear recoils produced by the neutrino-nucleus scattering events. Recently, CEνNS was detected by the COHERENT collaboration [2] thanks to the development of novel detectors and the unique neutrino beam facility of the Spallation Neutron Source (SNS) at the Oak Ridge National Laboratory.

The potential for CEνNS as a tool to search for new physics has been extensively discussed in the literature [3, 4]. More recently, data from COHERENT have opened a window into the low-energy neutrino sector. The COHERENT data imposed new constraints on non-standard neutrino interactions (NSI) [5, 6], and established new limits on sterile neutrino models [7, 8]. Other searches for new physics with COHERENT data are discussed in [9] and [10].

The COHERENT experiment explores the high-energy tail of CEνNS, using neutrinos with energies above 20 MeV in order to produce observable nuclear recoils in detectors with thresholds of the order of 20 keV. On the other hand, several efforts are ongoing to observe the CEνNS using neutrinos from nuclear reactors [11–14], with typical neutrino energy of around 1 MeV. However, the SM signal has not yet been detected due to the very low-energy nuclear recoil signals produced.

The Coherent Neutrino-Nucleus Interaction Experiment (CONNIE) [15] uses low-noise fully depleted charge-coupled devices (CCDs) [16] with the goal of measuring low-energy recoils from CEνNS produced by reactor antineutrinos with silicon nuclei [17]. The CONNIE

engineering run, carried out in 2014–2015, is discussed in [18]. The detector installed in 2016 has an active mass of 73.2 g (12 CCDs) and is located 30 m from the core of the Angra 2 nuclear reactor, which has a thermal power of 3.95 GW. The CONNIE detector explores recoil energies down to 1 keV. A search for neutrino events is performed by comparing data with the reactor on (2.1 kg-day) and the reactor off (1.6 kg-day), the results show no excess in the reactor-on data [19]. A model independent 95% Confidence Level (C.L.) limit for new physics was established at an event rate of ∼40 times the one expected from the SM at the lowest energies.

In this work we use the CONNIE results presented in [19] to constrain the parameter space for extensions of the SM containing a light, neutral vector boson Z', with mass $M_{Z'}$ that is comparable to the momentum transfer. Such extensions of the SM are of interest because there are no constraints from the Large Hadron Collider (LHC) when the mediator mass is below the GeV scale [9]. From the theoretical side, these models have attracted considerable attention because, among other things, they connect to new ideas associated with sub-GeV dark matter in the range of MeV to GeV [9, 20]. To keep things as simple as possible, we will assume that there is no Z-Z' mixing and that the Z' has a purely vector interaction with the fermions of the SM, with a universal flavor-conserving coupling to the first generation of quarks and leptons.

The paper is organized as follows. In Section 2, the event rate for CEνNS in CONNIE is calculated in both the SM and its extension with an additional light vector mediator. In Section 3, the results of the CONNIE experiment are used to establish a limit on the parameter space for the light vector mediator extension. Two appendices have been included with details of the neutrino flux and detector performance information needed to calculate the event rate. These details are published elsewhere and given here for completeness.

2 Event rate in CONNIE

The CEνNS interaction happens when the three-momentum transfer $q = |\mathbf{q}|$ is small enough so that $q^2R^2 < 1$, with R being the nuclear radius. In the laboratory frame, this corresponds to an energy of the incident antineutrino below 50 MeV. For reactor antineutrinos, the energies involved are below ∼5 MeV and the above condition is well satisfied. In the SM, the differential cross section for the coherent elastic scattering of antineutrinos off a nucleus at rest, with Z protons, N neutrons and mass M is given by

$$\frac{d\sigma_{SM}}{dE_R}(E_{\bar{\nu}_e}) = \frac{G_F^2}{8\pi}Q_W^2\left[2 - \frac{2E_R}{E_{\bar{\nu}_e}} + \left(\frac{E_R}{E_{\bar{\nu}_e}}\right)^2 - \frac{ME_R}{E_{\bar{\nu}_e}^2}\right]M|F(q)|^2\,, \tag{2.1}$$

where G_F is the Fermi coupling constant, $E_{\bar{\nu}_e}$ is the antineutrino energy, E_R is the nuclear recoil energy and

$$Q_W = N - (1 - 4\sin^2\theta_W)Z\,, \tag{2.2}$$

is the weak charge. Here, θ_W is the weak mixing angle and $F(q)$ is the nuclear form factor, which can be expressed as in [21] as

$$F(q) = \frac{4\pi\rho_0}{Aq^3}(\sin qR - qR\cos qR)\frac{1}{1+(aq)^2}\,, \tag{2.3}$$

where A is the atomic mass of the nucleus, $a = 0.7 \times 10^{-13}$ cm is the range of the Yukawa potential considered, $R = r_0 A^{1/3}$ is the nuclear radius and $\rho_0 = 3/4\pi r_0^3$ is the nuclear density, with $r_0 = 1.3 \times 10^{-13}$ cm being the average radius of a proton in a nucleus. At low energies, $\sin^2\theta_W = 0.23857$ [22].

Let us now take into consideration the non-standard interactions associated to a light vector mediator Z' with mass $M_{Z'}$ and coupling g'. At tree level, the net effect on the CEνNS is merely a modification of the global factor Q_W^2 in Eq. (2.4) [5]. Thus, the differential cross section now becomes:

$$\frac{d\sigma_{LM}}{dE_R}\left(E_{\bar{\nu}_e}\right) = \left(\frac{Q_{LM}}{Q_W}\right)^2 \frac{d\sigma_{SM}}{dE_R}\left(E_{\bar{\nu}_e}\right) , \tag{2.4}$$

where

$$Q_{LM} = Q_W - f_{LM}(E_R)\,(N+Z) , \tag{2.5}$$

with

$$f_{LM}\left(E_R\right) = \frac{3g'^2}{\sqrt{2}G_F\left(2ME_R + M_{Z'}^2\right)} . \tag{2.6}$$

In particular, for silicon nuclei ($N = Z = 14$), the expressions in Eqs. (2.2) and (2.5) reduce to $Q_W = 4N\sin^2\theta_W$ and $Q_{LM} = 2N\big(2\sin^2\theta_W - f_{LM}(E_R)\big)$, respectively.

The CEνNS event rate as a function of the nuclear recoil energy E_R in the CONNIE experiment is

$$\frac{dR}{dE_R} = N_T \int_{E_{\bar{\nu}_e}^{\min}}^{\infty} \frac{d\Phi}{dE_{\bar{\nu}_e}} \frac{d\sigma}{dE_R}\, dE_{\bar{\nu}_e} , \tag{2.7}$$

where $d\sigma/dE_R$ is the differential cross section (Eq. (2.1) or Eq. (2.4)), $d\Phi/dE_{\bar{\nu}_e}$ is the reactor antineutrino flux (discussed in Appendix A), N_T is the number of nuclei in the detector and $E_{\bar{\nu}_e}^{\min} = \left(E_R + \sqrt{E_R^2 + 2ME_R}\right)/2$ is the minimal antineutrino energy that can produce a nuclear recoil with energy E_R.

The CONNIE sensors detect the ionization produced by the recoiling silicon nuclei. As discussed in Appendix B, the quenching factor Q relates the ionizing energy E_I to the recoil energy: $E_R = E_I/Q(E_I)$. Taking this relation into account we get the differential event rate as a function of E_I,

$$\frac{dR}{dE_I} = \frac{dR}{dE_R}\frac{dE_R}{dE_I} = \frac{dR}{dE_R}\frac{1}{Q}\left(1 - \frac{E_I}{Q}\frac{dQ}{dE_I}\right) . \tag{2.8}$$

The total rate R in the CONNIE experiment is given by

$$R = \int_{E_{\rm th}}^{\infty} \epsilon(E_M)\, \frac{dR}{dE_M}\, dE_M , \tag{2.9}$$

where E_M is the measured energy, $\epsilon(E_M)$ denotes the reconstruction efficiency (see Appendix B) and $E_{\rm th} = 0.064$ keV is the detector threshold given by the efficiency curve. Assuming a Gaussian detector response, the differential event rate as a function of E_M is

$$\frac{dR}{dE_M} = \frac{\int_0^\infty G\left(E_M, E_I; \sigma_I^2\right) \frac{dR}{dE_I}\, dE_I}{\int_0^\infty G\left(E_M, E_I; \sigma_I^2\right) dE_I} , \tag{2.10}$$

where

$$G\left(E_M, E_I; \sigma_I^2\right) = \frac{1}{\sqrt{2\pi\sigma_I^2}} \exp\left\{-\frac{\left(E_M - E_I\right)^2}{2\sigma_I^2}\right\}, \tag{2.11}$$

with $\sigma_I^2 = (0.034 \text{ keV})^2 + F E_{\text{eh}} E_I$ characterizing the energy resolution of a typical CONNIE CCD [23]. Here, F is the Fano factor (0.133) and E_{eh} is the mean ionization energy required for photons to produce an electron-hole pair in silicon (0.003745 keV) [24].

3 Search for light vector mediator using CONNIE data

The results in the recent CONNIE run discussed in Ref. [19] establish new limits for the rate of low-energy antineutrino events coming from non-standard interactions R_{NSI} based on a comparison of reactor-on (RON) and reactor-off (ROFF) data. These limits are shown in Fig. 1, together with the expected event rate for the Standard Model, R_{SM}. From the lowest energy bin of this figure, we see that the 95% C.L. upper limit established by CONNIE is 41 times above the SM prediction using the measurements of quenching factor in Ref. [25]. This allows us to set the limit $R_{NSI} < R_{SM} \times 41$ for 0.075 keV $< E_M <$ 0.275 keV (or recoil energies 0.784 keV $< E_R <$ 1.834 keV). Here, we apply this limit on R_{NSI} in order to constrain a possible extension of the SM with a light vector mediator as described by Eq. (2.4). The 95% C.L. exclusion limits for the model parameters g' and $M_{Z'}$ are shown in Fig. 2. The most significant systematic uncertainty in this limit comes from the quenching factor measurement, as discussed in Ref. [19]. To quantify the effect of this uncertainty, we also include in Fig. 2 the exclusion region calculated using the quenching factor from Ref. [26].

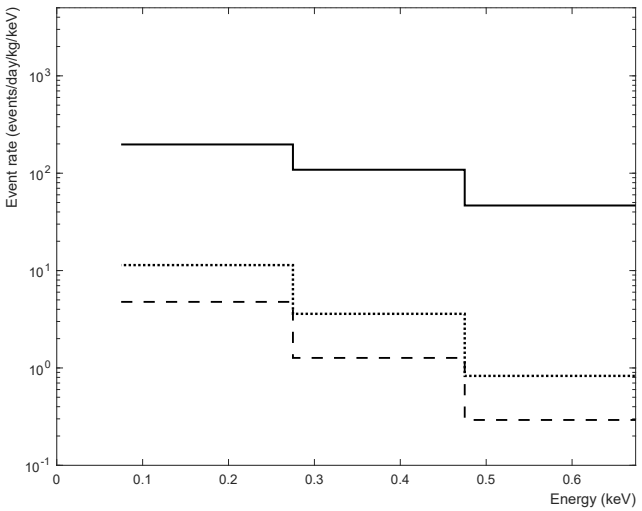

Figure 1. 95% confidence level limit from RON-ROFF measurements (solid line) and CEνNS expected event rate using measurements in Ref. [25] (dashed line) and expressions in Ref. [26] (dotted line) for the quenching factor. Figure from Ref. [19].

According to the expression in Eq. (2.4), the contribution of the additional vector mediator to the event rate is proportional to $g'^2/\left(2ME_R + M_{Z'}^2\right)$. Therefore, for a light

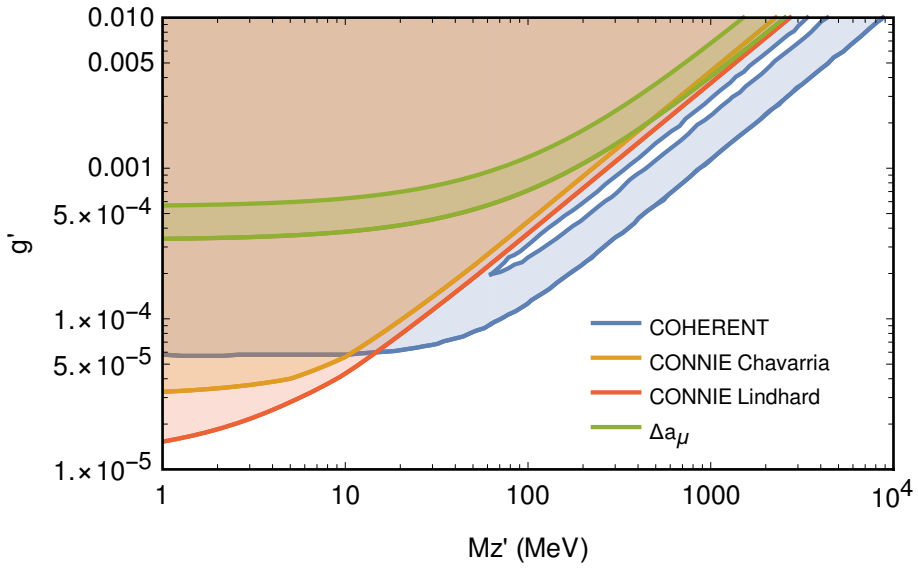

Figure 2. Exclusion region in the $(M_{Z'}, g')$ plane from the CONNIE results assuming quenching given by the fit to the measurements in Ref. [25] (orange) and the expressions in Ref. [26] (red). The COHERENT limit curve [5] (blue) and the 2σ allowed region to explain the anomalous magnetic moment of the muon ($\Delta a_\mu = 268 \pm 63 \times 10^{-11}$) [27, 28] (green) are shown for reference.

mediator, $M_{Z'} \ll \sqrt{2ME_R}$, the NSI contribution depends only on g' and the limit becomes independent of mass. For a heavy mediator, $M_{Z'} \gg \sqrt{2ME_R}$, the NSI rate contribution is proportional to the ratio $g'/M_{Z'}c^2$. These two regimes are visible in Fig. 2. Moreover, the CONNIE limit curve confirms the statement in Ref. [5], disfavoring a light vector mediator to explain the discrepancy in the anomalous magnetic moment of the muon.

4 Conclusion

We use the recent results of the CONNIE experiment [19] to examine the constraints on neutrino neutral-current interactions associated to a light vector-boson extension of the SM. As a result of this analysis, a new world-leading limit is established for the low-mass regime $M_{Z'} < 10$ MeV, extending beyond the region excluded by the COHERENT results [18].

This analysis demonstrates the power of combining a high flux of low-energy antineutrinos from a nuclear reactor with a low-threshold detector as a tool for exploring new physics. The results constitute the first search for NSI with reactor neutrinos and CCDs, and are expected to be the first in a series of searches using the CONNIE data.

Two features of the present study are expected to be improved in the future. The current analysis is based on a counting experiment, comparing the number of events above threshold in CONNIE with the expectations from a model with a light vector mediator. A more powerful limit is expected when spectral information of the CONNIE data is included in the analysis. Additionally, the CONNIE collaboration has recently modified the operation of the detector, performing hardware binning on the CCDs (adding charge of several pixels

before readout) and reducing the effect of readout noise for the low-energy events. This operating mode improves the efficiency of the detector at low energies. An updated result using data taken with this mode is expected soon.

A Reactor flux

The CONNIE detector is located 30 m from the core of the Angra 2 reactor of the Almirante Alvaro Alberto Nuclear Power Plant, in Rio de Janeiro, Brazil. The thermal power of this reactor is 3.95 GW $= 2.46 \times 10^{22}$ MeV/s. Considering that the average energy released per fission is 205.24 MeV, the number of fissions per second for this reactor is $n_f = 1.2 \times 10^{20}$.

The β decays of the fission products, following the fission of four principal fissile isotopes (^{235}U, ^{238}U, ^{239}Pu and ^{241}Pu), produce a large number of $\bar{\nu}_e$, contributing approximately 84% to the total reactor's antineutrino flux. Each fissile isotope has its own $\bar{\nu}_e$ spectrum, which has been taken from [29]. For energies below 2 MeV, the antineutrino spectra are given as tabulated values in Table 1, while for energies above 2 MeV these spectra are

$E_{\bar{\nu}_e}$(MeV)	^{235}U	^{239}Pu	^{238}U	^{241}Pu
7.813×10^{-3}	0.024	0.14	0.089	0.20
1.563×10^{-2}	0.092	0.56	0.35	0.79
3.12×10^{-2}	0.35	2.13	1.32	3.00
6.25×10^{-2}	0.61	0.64	0.65	0.59
0.125	1.98	1.99	2.02	1.85
0.25	2.16	2.08	2.18	2.14
0.50	2.66	2.63	2.91	2.82
0.75	2.66	2.58	2.96	2.90
1.0	2.41	2.32	2.75	2.63
1.5	1.69	1.48	1.97	1.75
2.0	1.26	1.08	1.50	1.32

Table 1. Tabulated values of the antineutrino spectrum of each fissile isotope in units of $\bar{\nu}_e$/MeV/fis.

described by the parametric expression

$$\frac{dN_{\bar{\nu}_e}}{dE_{\bar{\nu}_e}} = a e^{a_0 + a_1 E_{\bar{\nu}_e} + a_2 E_{\bar{\nu}_e}^2}, \tag{A.1}$$

where the fitted parameters are listed in Table 2.

Another process that contributes approximately 16% to the reactor antineutrino flux is the neutron capture of ^{238}U nuclei. These nuclei capture 0.6 neutrons per fission via the reaction ^{238}U + n $\rightarrow^{239}$U $\rightarrow^{239}$Np $\rightarrow^{239}$ Pu. The β decay of ^{239}U produces two $\bar{\nu}_e$. The antineutrino spectrum of this process was extracted from [30].

Each process previously considered has its own $\bar{\nu}_e$ yield and fission rate. The respective values were taken from [30] and are shown in Table 3.

Parameter	^{235}U	^{239}Pu	^{238}U	^{241}Pu
a	1.0461	1.0527	1.0719	1.0818
a_0	0.870	0.896	0.976	0.793
a_1	−0.160	−0.239	−0.162	−0.080
a_2	−0.0910	−0.0981	−0.0790	−0.1085

Table 2. Fitted parameters of the antineutrino spectrum of each fissile isotope.

Process	Relative rate per fission	$N_{\bar{\nu}_e}$ per process	$N_{\bar{\nu}_e}$ per fission
^{235}U fission	0.55	6.14	3.4
^{239}Pu fission	0.32	5.58	1.8
^{238}U fission	0.07	7.08	0.5
^{241}Pu fission	0.06	6.42	0.4
$^{238}\mathrm{U}(n,\gamma)^{239}\mathrm{U}$	0.60	2.00	1.2

Table 3. Typical relative fission contribution and $\bar{\nu}_e$ yield for each process considered [30].

In order to obtain the total antineutrino reactor spectrum per fission per MeV, $d\mathcal{N}_{\bar{\nu}_e}/dE_{\bar{\nu}_e}$, the individual spectra were summed after being normalized and multiplied by their corresponding $\bar{\nu}_e$ yield per fission.

The total antineutrino flux, i.e. the number of antineutrinos per MeV per cm^2 per second, crossing the CONNIE detector is given by

$$\frac{d\Phi}{dE_{\bar{\nu}_e}} = \frac{n_f}{4\pi d^2}\left(\frac{d\mathcal{N}_{\bar{\nu}_e}}{dE_{\bar{\nu}_e}}\right), \tag{A.2}$$

where $d = 30 \times 10^2$ cm is the distance between the reactor and the detector. The flux expected at the CONNIE detector is shown in Fig. 3.

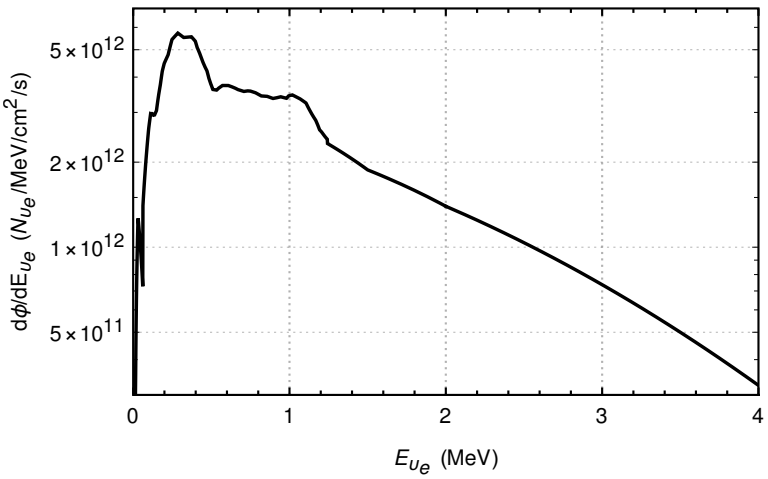

Figure 3. Antineutrino flux expected at the CONNIE detector.

B Fitting functions for quenching factor and efficiency

When a nuclear recoil is produced inside the detector, a part of its energy generates charge carriers (E_I) and the rest contributes to the increase of the thermal energy of the system. The nuclear recoil quenching factor Q is defined as the fraction of the total recoil energy E_R that is used to produce ionization

$$Q = E_I/E_R\,. \tag{B.1}$$

For $E_R \gtrsim 4$ keV, the nuclear recoil quenching factor is well modelled by Lindhard [26]. Two measurements of the quenching factor for E_R below 4 keV were performed using similar detectors in different experiments [25, 31]. An analytical fit to the measurements in [25] is used here, parametrized as

$$Q(E_I) = \frac{p_3 E_I + p_4 E_I^2 + E_I^3}{p_0 + p_1 E_I + p_2 E_I^2}\,, \tag{B.2}$$

with $p_0 = 56$ keV^3, $p_1 = 1096$ keV^2, $p_2 = 382$ keV, $p_3 = 168$ keV^2 and $p_4 = 155$ keV, as shown in Fig. 4.

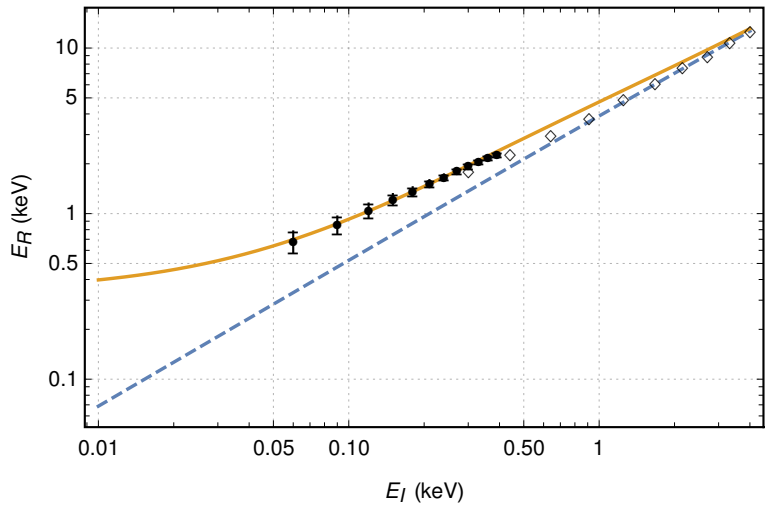

Figure 4. Nuclear recoil quenching factors: Lindhard [26] (dashed blue line), measurements in [31] (◇) and in [25] (●) and fit described by Eq. (B.2) (solid orange line).

In order to extract and reconstruct the events registered during a CCD exposure, a set of processing tools is used. The reconstruction efficiency for these tools has been evaluated in Ref. [19] using simulated events. The computed efficiency is fitted well for $E_M > 64$ eV by

$$\epsilon(E_M) = b - \left[1 + e^{b_0(E_M - b_1)}\right]^{-1}\,, \tag{B.3}$$

where $b = 0.7426$, $b_0 = 17.47$ and $b_1 = 0.1239$, as shown in Fig. 5.

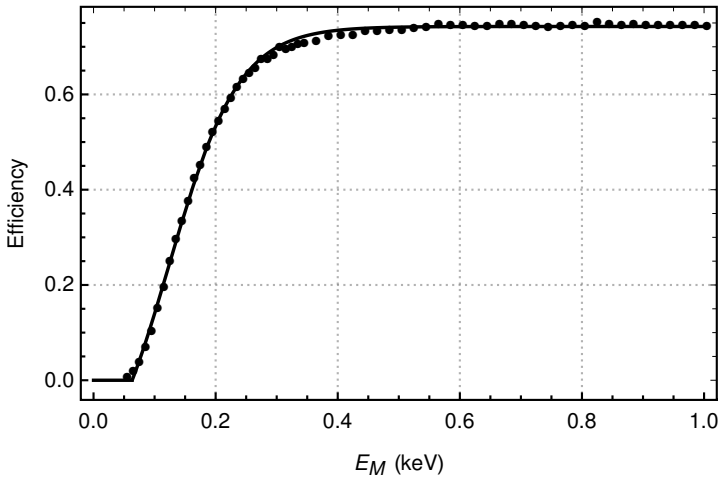

Figure 5. Processing efficiency for CONNIE data obtained from simulated events [19] (•) and the fit described by Eq. (B.3) (solid line).

Acknowledgments

We thank Eletrobras Eletronuclear for access to the Angra 2 reactor site and for the support of their personnel, in particular Ilson Soares and Gustavo Coelho, to the CONNIE activities. We thank the Silicon Detector Facility team at Fermi National Accelerator Laboratory for being the host lab for the assembly and testing of the detectors components used in the CONNIE experiment. We acknowledge the support from the former Brazilian Ministry for Science, Technology, and Innovation (currently MCTIC), the Brazilian Center for Physics Research and the Brazilian funding agencies FAPERJ (grants E-26/110.145/2013, E-26/210.151/2016), CNPq, and FINEP (RENAFAE grant 01.10.0462.00); and México's CONACYT (grant No. 240666) and DGAPA-UNAM (PAPIIT grant IN108917).

References

[1] D. Z. Freedman, *Coherent effects of a weak neutral current*, *Phys. Rev. D* **9** (Mar, 1974) 1389–1392.

[2] **COHERENT** Collaboration, D. Akimov et al., *Observation of Coherent Elastic Neutrino-Nucleus Scattering*, *Science* **357** (2017), no. 6356 1123–1126, [arXiv:1708.01294].

[3] R. Harnik, J. Kopp, and P. A. N. Machado, *Exploring ν signals in dark matter detectors*, *JCAP* **1207** (2012) 026, [arXiv:1202.6073].

[4] J. Billard, J. Johnston, and B. J. Kavanagh, *Prospects for exploring New Physics in Coherent Elastic Neutrino-Nucleus Scattering*, *JCAP* **1811** (2018) 016, [arXiv:1805.01798].

[5] J. Liao and D. Marfatia, *COHERENT constraints on nonstandard neutrino interactions*, *Phys. Lett.* **B775** (2017) 54–57, [arXiv:1708.04255].

[6] D. Aristizabal Sierra, V. De Romeri, and N. Rojas, *COHERENT analysis of neutrino generalized interactions*, *Phys. Rev.* **D98** (2018) 075018, [arXiv:1806.07424].

[7] T. S. Kosmas, D. K. Papoulias, M. Tortola, and J. W. F. Valle, *Probing light sterile neutrino signatures at reactor and Spallation Neutron Source neutrino experiments*, *Phys. Rev.* **D96** (2017) 063013, [arXiv:1703.00054].

[8] C. Blanco, D. Hooper, and P. Machado, *Constraining Sterile Neutrino Interpretations of the LSND and MiniBooNE Anomalies with Coherent Neutrino Scattering Experiments*, *arXiv e-prints* (2019) [arXiv:1901.08094].

[9] B. Dutta, S. Liao, S. Sinha, and L. E. Strigari, *Searching for beyond the standard model physics with coherent energy and timing data*, *Phys. Rev. Lett.* **123** (2019) 061801, [arXiv:1903.10666].

[10] O. G. Miranda, D. K. Papoulias, M. Tórtola, and J. W. F. Valle, *Probing neutrino transition magnetic moments with coherent elastic neutrino-nucleus scattering*, *JHEP* **07** (2019) 103, [arXiv:1905.03750].

[11] D. Y. Akimov et al., *RED-100 detector for the first observation of the elastic coherent neutrino scattering off xenon nuclei*, *J. Phys. Conf. Ser.* **675** (2016) 012016.

[12] **MINER** Collaboration, G. Agnolet et al., *Background Studies for the MINER Coherent Neutrino Scattering Reactor Experiment*, *Nucl. Instrum. Meth.* **A853** (2017) 53–60, [arXiv:1609.02066].

[13] J. Billard et al., *Coherent Neutrino Scattering with Low Temperature Bolometers at Chooz Reactor Complex*, *J. Phys.* **G44** (2017) 105101, [arXiv:1612.09035].

[14] J. HakenmÃijller et al., *Neutron-induced background in the CONUS experiment*, *Eur. Phys. J.* **C79** (2019) 699, [arXiv:1903.09269].

[15] **CONNIE** Collaboration, A. Aguilar-Arevalo et al., *The CONNIE experiment*, *J. Phys. Conf. Ser.* **761** (2016) 012057, [arXiv:1608.01565].

[16] S. E. Holland, D. E. Groom, N. P. Palaio, R. J. Stover, and M. Wei, *Fully depleted, back-illuminated charge-coupled devices fabricated on high-resistivity silicon*, *IEEE Transactions on Electron Devices* **50** (Jan, 2003) 225–238.

[17] G. Fernandez Moroni, J. Estrada, E. E. Paolini, G. Cancelo, J. Tiffenberg, and J. Molina, *Charge Coupled Devices for detection of coherent neutrino-nucleus scattering*, *Phys. Rev.* **D91** (2015) 072001, [arXiv:1405.5761].

[18] **CONNIE** Collaboration, A. Aguilar-Arevalo et al., *Results of the Engineering Run of the Coherent Neutrino Nucleus Interaction Experiment (CONNIE)*, *JINST* **11** (2016) P07024, [arXiv:1604.01343].

[19] **CONNIE** Collaboration, A. Aguilar-Arevalo et al., *Exploring Low-Energy Neutrino Physics with the Coherent Neutrino Nucleus Interaction Experiment (CONNIE)*, *arXiv e-prints* (2019) [arXiv:1906.02200]. [Accepted for publication in PRD].

[20] R. Essig, J. A. Jaros, and W. Wester, *Dark Sectors and New, Light, Weakly-Coupled Particles*, 2013.

[21] S. R. Klein and J. Nystrand, *Interference in exclusive vector meson production in heavy ion collisions*, *Phys. Rev. Lett.* **84** (2000) 2330–2333, [hep-ph/9909237].

[22] **Particle Data Group** Collaboration, M. Tanabashi et al., *Review of particle physics*, *Phys. Rev. D* **98** (Aug, 2018) 030001.

[23] **DAMIC** Collaboration, A. Aguilar-Arevalo et al., *Search for low-mass WIMPs in a 0.6 kg day exposure of the DAMIC experiment at SNOLAB*, *Phys. Rev.* **D94** (2016) 082006, [arXiv:1607.07410].

[24] R. D. Ryan, *Precision measurements of the ionization energy and its temperature variation in high purity silicon radiation detectors*, *IEEE Transactions on Nuclear Science* **20** (Feb, 1973) 473–480.

[25] A. E. Chavarria et al., *Measurement of the ionization produced by sub-keV silicon nuclear recoils in a CCD dark matter detector*, *Phys. Rev.* **D94** (2016) 082007, [arXiv:1608.00957].

[26] J. Lindhard, M. Scharff, and H. Schioett, *Range concepts and heavy ion ranges (Notes on atomic collisions, II)*, *Kgl. Danske Videnskab. Selskab. Mat. Fys. Medd.* **33** (1963), no. 14.

[27] F. Jegerlehner and A. Nyffeler, *The Muon g-2*, *Phys. Rept.* **477** (2009) 1–110, [arXiv:0902.3360].

[28] N. V. Krasnikov, *Light scalars, $(g_\mu - 2)$ muon anomaly and dark matter in a model with a Higgs democracy*, *arXiv e-prints* (2017) [arXiv:1707.00508].

[29] P. Vogel and J. Engel, *Neutrino Electromagnetic Form-Factors*, *Phys. Rev.* **D39** (1989) 3378.

[30] **TEXONO** Collaboration, H. T. Wong et al., *A Search of Neutrino Magnetic Moments with a High-Purity Germanium Detector at the Kuo-Sheng Nuclear Power Station*, *Phys. Rev.* **D75** (2007) 012001, [hep-ex/0605006].

[31] F. Izraelevitch et al., *A Measurement of the Ionization Efficiency of Nuclear Recoils in Silicon*, *JINST* **12** (2017) P06014, [arXiv:1702.00873].